

# Comparison of Gravitational and Light Frequency Shifts in Rubidium Atomic Clock

Alexey Baranov, Sergey Ermak \*, Roman Lozov and Vladimir Semenov

The Institute of Physics, Nanotechnology and Telecommunications, Peter the Great St. Petersburg Polytechnic University, 195251 Saint Petersburg, Russia; 79111700994@ya.ru (A.B.); lozov-rk@ya.ru (R.L.); vladimir\_semenov@mail.ru (V.S.)

\* Correspondence: serge\_ermak@mail.ru; Tel.: +7-921-791-9091

**Abstract:** The article presents the results of an experimental study of the external magnetic field orientation and magnitude influence on the rubidium atomic clock, simulating the influence of the geomagnetic field on the onboard rubidium atomic clock of navigation satellites. The tensor component value of the atomic clock frequency light shift on the rubidium cell was obtained, and this value was  $\sim 2$  Hz. The comparability of the relative light shift ( $\sim 10^{-9}$ ) and the regular gravitational correction ( $4 \times 10^{-10}$ ) to the frequency of the rubidium atomic clock was shown. The experimental results to determine the orientational shift influence on the rubidium atomic clock frequency were presented. A significant effect on the relative frequency instability of a rubidium atomic clock at a level of  $10^{-12}$  ( $10^{-13}$ ) for rotating external magnetic field amplitudes of 1.5 A/m and 3 A/m was demonstrated. This magnitude corresponds to the geomagnetic field in the orbit of navigation satellites. The necessity of taking into account various factors (satellite orbit parameters and atomic clock characteristics) is substantiated for correct comparison of corrections to the rubidium onboard atomic clock frequency associated with the Earth's gravitational field action and the satellite orientation in the geomagnetic field.

**Keywords:** rubidium atomic clocks; light shift; navigation satellites



**Citation:** Baranov, A.; Ermak, S.; Lozov, R.; Semenov, V. Comparison of Gravitational and Light Frequency Shifts in Rubidium Atomic Clock. *Universe* **2021**, *7*, 3. <https://dx.doi.org/10.3390/universe7010003>

Received: 15 September 2020

Accepted: 19 December 2020

Published: 24 December 2020

**Publisher's Note:** MDPI stays neutral with regard to jurisdictional claims in published maps and institutional affiliations.



**Copyright:** © 2020 by the authors. Licensee MDPI, Basel, Switzerland. This article is an open access article distributed under the terms and conditions of the Creative Commons Attribution (CC BY) license (<https://creativecommons.org/licenses/by/4.0/>).

## 1. Introduction

The general theory of relativity (GTR) has found its confirmation in numerous experiments, where a high-precision atomic clock plays a central role, in which the relative error does not exceed  $10^{-14}$ . A typical example of such experiments are the results published in Reference [1], where the atomic clock time shift (hydrogen maser clock) of two Galileo system navigation satellites was investigated. The satellites were launched into elliptical orbits with an eccentricity of  $\varepsilon \approx 0.162$  and an orbital period of  $\sim 13$  h. As a result, it was found that the redshifts relative deviation between predicted by GTR and measured in practice differs by no more than  $(0.19 \pm 2.5) \cdot 10^{-5}$ . In this case, the gravitational shift in time of the atomic clock relative to the reference analogue on Earth experienced up to 200 ns periodic variations.

Taking into account relativistic effects, according to GTR, the relative difference in frequencies of atomic clocks installed in the navigation satellites onboard equipment and installed on Earth can be estimated in accordance with the expression obtained using the data of the article [2]:

$$\frac{\Delta f_1}{f} = -\frac{1}{c^2} \left( \frac{v_2^2 - v_1^2}{2} + \left( \frac{GM}{R+h} - \frac{GM}{R} \right) \right), \quad (1)$$

where  $v_1$  and  $v_2$  are the speeds of the atomic clock in a geocentric non-rotating coordinate system in the orbit and on the Earth's surface respectively,  $c$  is the speed of light,  $G$  is the

gravitational constant,  $M$  is the Earth's mass,  $R$  is the Earth average radius, and  $h$  is the satellite height above the Earth's surface.

Expression (1) can be used to calculate the regular correction to the time scale of the atomic clock, which is automatically taken into account when tuning the onboard frequency synthesizer. With  $R = 6400$  km and a fixed altitude for navigation satellites  $h = 20,000$  km, the relative frequency shift calculated by formula (1) is  $4 \times 10^{-10}$ . However, in practice, the parameter  $h$  does not remain constant, as the orbits of satellites of various navigation systems, as a rule, have the shape of an ellipse (with an eccentricity  $\varepsilon$  from 0.001 to 0.1), which inevitably leads to change the onboard atomic clock time scale and, therefore, leads to the corresponding measurement error. The dependence of this time variation is easy to obtain from (1) knowing the satellite altitude at perigee  $h_P$  and apogee  $h_A$  of the elliptical orbit:

$$\frac{\Delta f}{f} = \frac{GM(h_A - h_P)}{2c^2(R + h_A)(R + h_P)}. \quad (2)$$

For satellites of the Galileo system with an average orbital altitude of 23,000 km with an eccentricity of 0.16 and a difference  $h_A - h_P = 8500$  km, the amplitude value of the atomic clock time shift for 6 h of observation calculated by formula (2) is  $\pm 300$  ns, which coincides as order of magnitude with the results of work in Reference [1]. The calculated value of the onboard atomic clock time shift is  $\sim 30$  ns for navigational system GLONASS with satellite orbits parameter of  $\varepsilon = 0.016$  and the average satellite altitude of 19,100 km. The above estimates show that the ephemeris error of navigation satellites systems associated with this relativistic effects influence: it is directly dependent on the orbit eccentricity. This dependence extends to all types of atomic clocks, among which small-sized versions based on optically pumped rubidium vapor play an important role [3]. The main source of errors in such devices is the so-called light shift of the resonance frequency, caused by the action of the non-resonant pumping light components on the working substance atoms. This light shift is due to the shift of the energy levels of the atom in the field of the light wave, associated with the dynamic Stark effect [4]. For alkali metal atoms, the light shift value is the sum of two components (scalar  $\Delta\nu_0$  and tensor  $\Delta\nu_T$ ), a characteristic feature of which is its dependence on the angle  $\theta$  between the external magnetic field direction and the pump light beam direction. This dependence is proportional to the  $\alpha \times (1 - 3 \cos^2 \theta)$ , where  $\alpha$  is the scale coefficient of the tensor component [5]. The variations of  $\theta$  for onboard atomic clock can lead to orientation errors of the navigation satellites comparable to the errors determined by formula (2). In this work, the above errors are compared on the basis of experiments that simulate the movement of navigation satellites onboard equipment.

## 2. Orientational Frequency Shift Investigation

The experimental estimate of the frequency light shift of a rubidium atomic clock on a gas cell was carried out with the laboratory setup described in Figure 1 and in the paper of Reference [6] and according to the method of Reference [7]. In this paper, we confirmed the results of the light shift tensor component study [7], carried out under the conditions, corresponding to the onboard arrangement of a rubidium atomic clock.

A cylindrical cell (1 cm in diameter and 1.5 cm in length with an anti-relaxation polyethylene wall coating) with a buffer gas (argon) from a rubidium atomic clock on a gas cell was used as a resonance cell. A horn antenna was used to provide the microwave field at the location of the gas cell. The antenna was oriented in such a way as to excite 0-0 resonant transitions in the variants of coaxial and orthogonal orientation of the external magnetic field with respect to the pump beam. In this case, both  $\pi$  and  $\sigma$  transitions are excited. While the magnitude of the  $\pi$  and  $\sigma$  transitions changed as the magnetic field orientation varied, the overall spectrum of the  $\pi$  and  $\sigma$  transitions remained unaltered. The optical path of the discriminator was placed at the center of three identical pairs of Helmholtz coils (diameter each is 50 cm), which created a working magnetic field in the gas cell area. Helmholtz coils were connected to AC power sources to create a rotating magnetic field relative to the normal to the direction of the pumping light. To weaken

external magnetic noise and inhomogeneities of the laboratory magnetic field, the entire system was placed in a two-layer magnetic screen with a screening coefficient of  $\sim 10^3$ . When detecting the radio-optical resonance signal, the traditional method of synchronous detection was used. The experiments were carried out at fixed intensities of the pump source ( $\sim 100 \mu\text{W}/\text{cm}^2$ ) controlled by neutral filters, which made it possible to measure the value of the light shift tensor component) [7]. The tensor component was determined from the resonance frequency shift under the conditions of magnetic field vector rotation ( $\sim 0.8 \text{ A/m}$ ) relative to the optical axis normal. Separate experiments [7] showed that the measured frequency shifts were proportional to the light intensity and independent of the magnetic-field magnitude. An example of such a dependence is shown in Figure 2 (the tensor component magnitude of the light shift at rotation angles from  $180^\circ$  to  $360^\circ$  has values corresponding to the rotation angles from  $0^\circ$  to  $180^\circ$ ) [7]. In Figure 2, the experimental value of the parameter  $\alpha$  is  $\approx 2 \text{ Hz}$ .

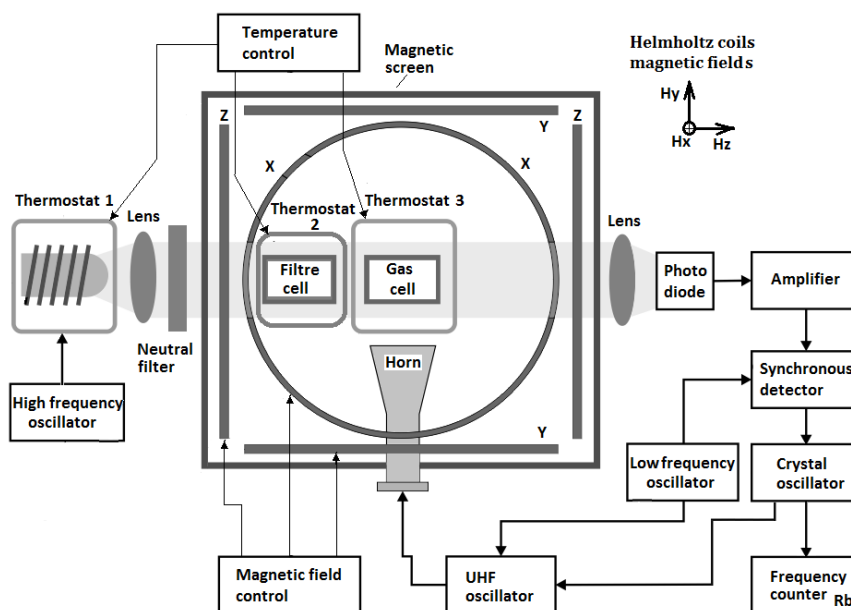


**Figure 1.** Laboratory setup used to study the frequency light shift in a rubidium atomic clock. The frequency counter is synchronized by rubidium atomic clock.

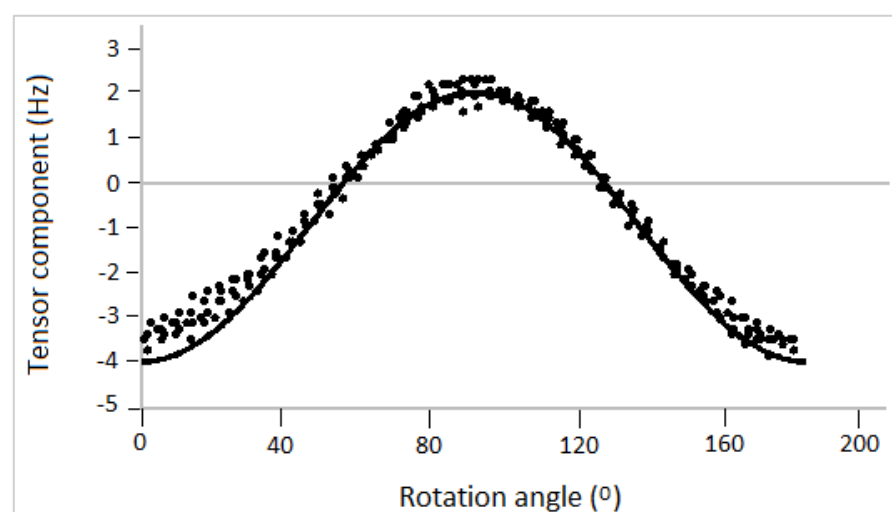


**Figure 2.** Orientation dependences of the 0-0 resonance frequency on the angle  $\theta$  at a light intensity of  $100 \mu\text{W}/\text{cm}^2$  (the dots indicate the experimental values of the orientational shift) [7].

The data (obtained in the experiment) correspond to the relative frequency light shift of atomic standards on rubidium vapor at a level of  $\sim 10^{-9}$ . Thus, in order to ensure the relative frequency instability at the level of  $10^{-13}$ , it is necessary to ensure the stability of the pump source intensity not worse than 0.01%, which corresponds to the conclusions of [8–10]. In order of magnitude, the above value of the relative light shift ( $\sim 10^{-9}$ ) is comparable to the regular correction ( $4 \times 10^{-10}$ ) associated with the gravity influence in accordance with formula (1). However, such a shift does not take into account the change of the onboard atomic clock frequency associated with the variation angle  $\theta$  when the satellite moves in orbit. Under the operating conditions of the onboard rubidium atomic clock, the presence of a magnetic screen significantly reduces the angle variation  $\theta$  between the atomic clock optical axis and the operating magnetic field direction. These variations are caused not only by a change in the magnitude and direction of the external geomagnetic field when the satellite moves in orbit, but also by a significant difference in the axial and transverse screening coefficients of the magnetic screen [11]. On the other hand, the absolute value of the geomagnetic field at the satellite orbit (with a strength of less than 0.6 A/m) is almost two magnitude orders less than the field strength on the planet's surface, which significantly reduces the efficiency of magnetic screening due to the weakening of the screen material magnetic permeability as the external magnetic field decreases. As in the experiments shown with a laboratory rubidium atomic clock, the orientational frequency shift value does not depend on the strength of the external magnetic field but is determined by the pumping rate and the atomic clock orientation in the geomagnetic field [7]. This orientation change when the satellite moves in orbit should inevitably lead to orientation errors in real onboard atomic clocks. To verify this statement in authors experiments, authors used two commercial small-sized atomic clocks on rubidium vapor (No. 1 and No. 2), manufactured by Frequency Electronics (model FE-5650A). The Allan deviation value of these devices during the averaging time of 100 s is less than  $1.4 \times 10^{-12}$ . The laboratory setup used to investigate the orientational frequency shift of the rubidium atomic clock is represented in Figure 3.

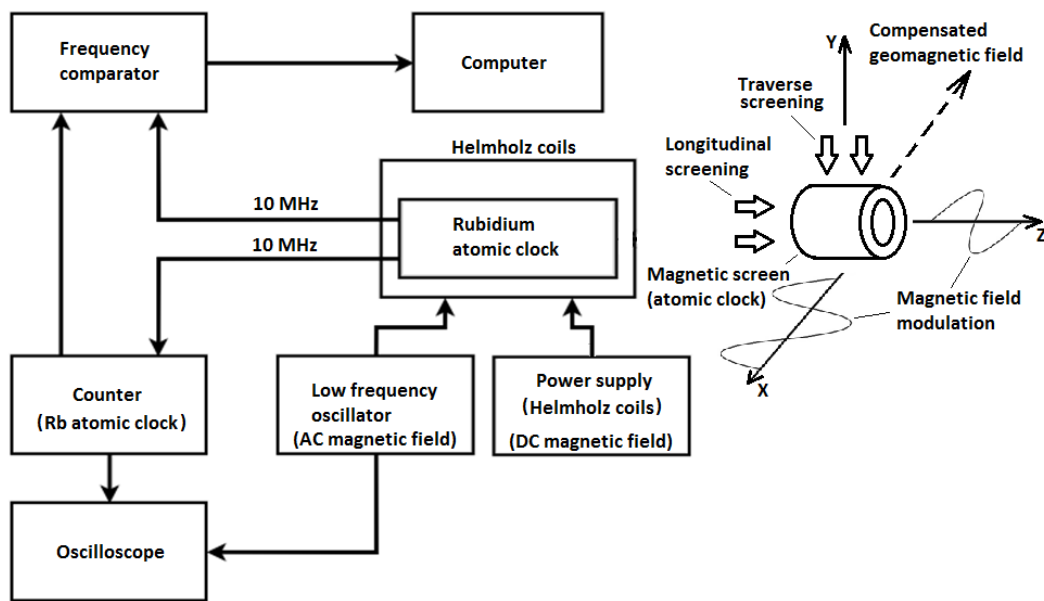


Figure 3. Laboratory setup used to study the orientational frequency shift of the rubidium atomic clock.

The atomic clock was placed in the center of three pairs of Helmholtz coils, which were used to geomagnetic field components compensation and create an artificial magnetic field, the direction of which could be varied relative to the atomic clock optical axis. To estimate the static screening coefficient of their magnetic screen, the current direction periodic switching in the Helmholtz coils was used, and the frequency of atomic clocks no. 1 and no. 2 was registered. As an example, Figure 4 shows the records of the atomic clock frequency variations for the case of current inversion in the Helmholtz coils, which created an artificial magnetic field  $H_{EXT}$  (75 A/m and zero field) along the atomic clock optical axis.

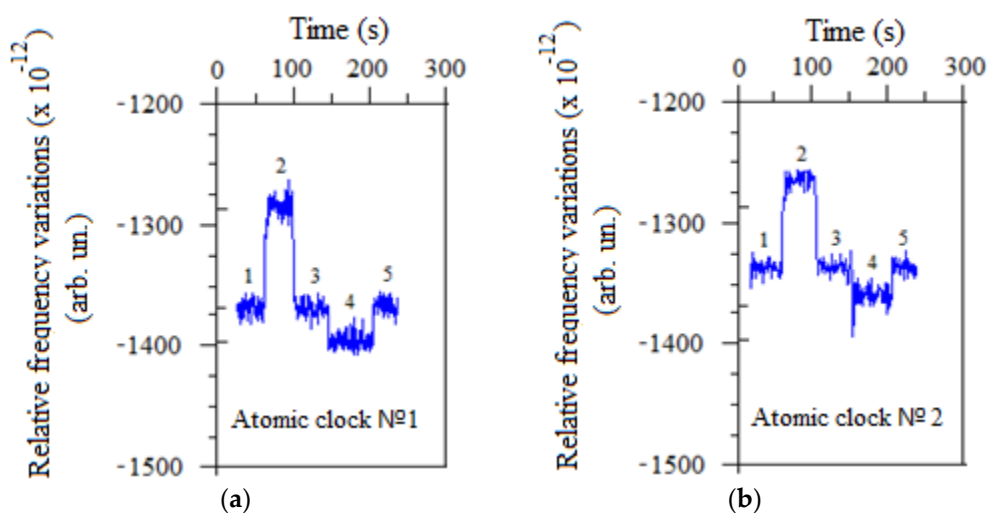


Figure 4. Recording of the atomic clock frequency variations in an external magnetic field created along their optical axis. Time sections 1, 2, 3, 4, and 5 correspond to the external magnetic field intensity  $H_{EXT}$  equal to 0, +75 A/m, 0, -75 A/m, 0: (a) atomic clock no. 1; (b) atomic clock no. 2.

The dependencies shown in Figure 4 allow to estimate the static screening coefficient along the axis of the atomic clock screen and the operating magnetic field magnitude inside the screen. By the well-known 0-0 resonance frequency dependence on the magnetic field

(with a coefficient at a quadratic term in the field of  $0.09 \frac{\text{Hz}}{(\text{A/m})^2}$ ) for rubidium atoms [12], it is easy to determine the static screening coefficient  $k$  and the value of the operating magnetic field strength  $H_{\text{IN}}$  inside atomic clock screen. For example, for an external magnetic field of 75 A/m, these parameters are estimated as follows:  $k \approx 90$  and  $H_{\text{IN}} \approx 2.64$  A/m (for atomic clock No. 1);  $k \approx 70$ ,  $H_{\text{IN}} \approx 2.16$  A/m (for atomic clock No. 2). The discrepancy between the obtained values of  $k$  and  $H_{\text{IN}}$  can be explained by the difference in the remnant magnetization degree of the atomic clock magnetic screens.

### 3. Magnetic Field Influence on the Atomic Clock Frequency Stability

The experiments simulating the geomagnetic field influence on the atomic clock readings when a satellite moves in orbit were carried out with laboratory setup (Figure 3) under conditions of a slowly varying external magnetic field (circular rotation of the magnetic field vector in the horizontal plane, where the atomic clock optical axis is located, with a frequency of 10.9 mHz and a sinusoidal waveform of a modulating signal). Figure 5 shows examples of time dependencies of the Allan deviation for atomic clock No. 1 at the rotating field amplitude values of 1.5 A/m (Figure 5a) and 3 A/m (Figure 5b), corresponding in order of magnitude to the value of the geomagnetic field at the satellite orbit. It should be noted that the rotating external magnetic field was chosen to demonstrate the influence of the geomagnetic field orientation on the onboard atomic clock. In the absence of external magnetic field modulation, the relative frequency instability of atomic clock No. 1 with averaging time up to 1000 s is well described by the dependence  $5.9 \times 10^{-12} / \tau^{1/2}$  (Figure 5, dotted lines,  $\tau$  is averaging time).

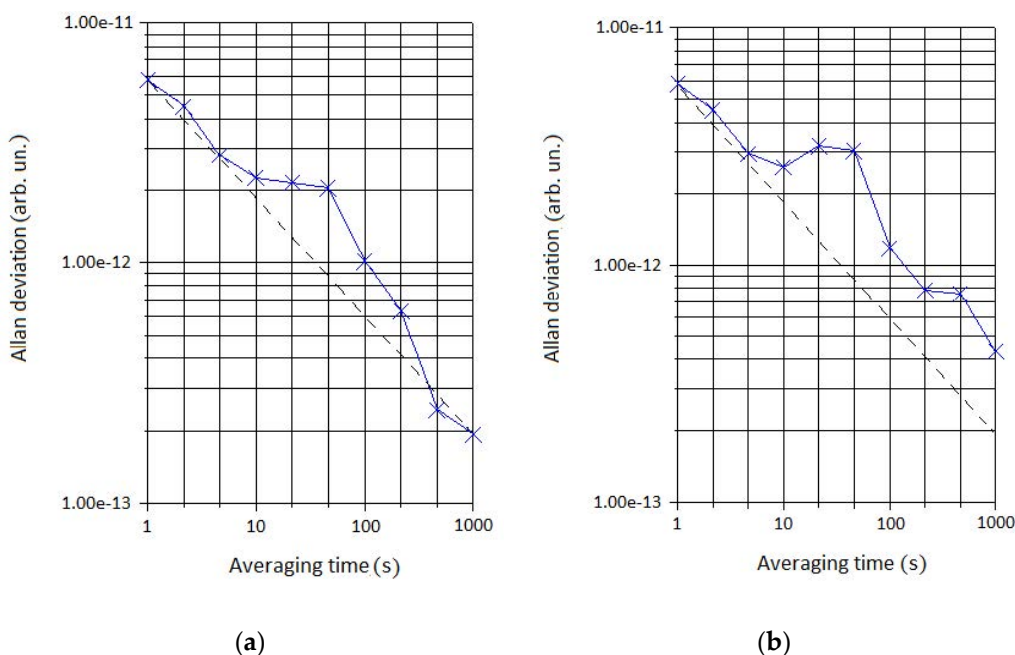


**Figure 5.** Orientation dependences of the 0-0 resonance frequency on the angle  $\theta$  (the dots indicate the experimental values of the orientational shift). Allan deviation dependence of atomic clock No. 1 on the averaging time (dotted line—Allan deviation for atomic clock No. 1 without external magnetic field modulation): (a) with magnetic field modulation with an amplitude of 1.5 A/m along the Z (phase shift  $0^\circ$ ) and X (phase shift  $90^\circ$ ) axes; (b) with modulation of the magnetic field with an amplitude of 3 A/m along the Z (phase shift  $0^\circ$ ) and X (phase shift  $90^\circ$ ) axes.

As follows from the dependencies shown in Figure 5, a periodic change in the external magnetic field direction corresponding to the geomagnetic field value at the orbit of navigation satellites leads to an increase in the relative frequency instability of the atomic clock by  $1.1 \times 10^{-12}$  (for the dependence in Figure 5a), by  $2.15 \times 10^{-12}$  (for the dependence in Figure 5b at 50 s averaging), and by  $2.3 \times 10^{-13}$  (for the dependence in Figure 5b at 1000 s



averaging), that can significantly affect positioning accuracy. The dependences presented in Figure 5 demonstrate the influence of magnetic fields varying in magnitude and direction on the frequency of the rubidium atomic clock. This result allows us to make a preliminary conclusion about the influence of the geomagnetic field on the onboard rubidium atomic clock of navigation satellites.

#### 4. Conclusions

A correct comparison of the influence of gravitational and geomagnetic fields on the atomic clock accuracy requires the elimination of third-party factors associated, for example, with solar activity. On the other hand, in a calm magnetic environment, when the unpredictable influence of geomagnetic field strong fluctuations is excluded, when gravitational and geomagnetic components of the atomic clock time shift are analyzed, it is necessary to take into account the correlation of their readings due to the external factors recurrence during the period of satellite movement in orbit. In this case, the reliability of the result of such analysis depends on the exact knowledge of the satellite orbit eccentricity, the screening properties of the used atomic clock magnetic screen and the operating magnetic field magnitude inside it, the intensity and spectral composition of the pumping source, and the parameters of the gas cell and the filter cell. The indicated difficulties in obtaining a reliable analysis result force us to resort to a qualitative assessment of such an influence. Nevertheless, the estimates obtained make it possible to predict the conditions under which there is an approximate measured frequency variations balance associated with the gravitational and orientation dependences of the atomic clock readings at the satellite orbit. For example, the experimental data obtained with a laboratory rubidium atomic clock, a variation of the angle  $\theta$  within  $1^\circ$  during the satellite flight within 100 s leads to an atomic onboard clock time shift at a level of 0.01 ns, which coincides in order of magnitude with the time shift for of the atomic clock on the GLONASS satellite with the parameter  $\varepsilon = 0.0016$ .

The experiments performed allow us to make a preliminary conclusion about the influence of a periodic external magnetic field orientation change (similar to the geomagnetic field at the orbit of a navigation satellite) on the frequency of an atomic clock with a rubidium cell. The experimentally measured value of the tensor component  $\Delta\nu_T$  corresponds to the relative shift of the rubidium atoms resonance frequency at a level of  $\sim 10^{-9}$ , which necessitates taking into account the orientational error of the onboard atomic clock. The experiments with commercial frequency standards have shown that geomagnetic field variations in satellite orbit limit the relative stability of the onboard atomic clock to values of  $10^{-12}$  for averaging times up to 1000 s. The results obtained can be used in the development of methods for improving the accuracy of satellite positioning systems [13–20].

**Author Contributions:** Conceptualization, V.S. and S.E.; methodology, V.S.; software, R.L.; validation, V.S., S.E. and A.B.; formal analysis, V.S.; investigation, S.E.; resources, S.E.; data curation, A.B.; writing—original draft preparation, V.S.; writing—review and editing, S.E.; visualization, S.E.; supervision, S.E.; project administration, S.E.; funding acquisition, S.E. All authors have read and agreed to the published version of the manuscript.

**Funding:** This research was funded by Russian Science Foundation, grant number 20-19-00146.

**Data Availability Statement:** The data presented in this study are available in [Ermak, S.V.; Lozov, R.K.; Semenov, V.V. Orientational Light Shift Experimental Estimate of 0-0 Resonance Frequency in Rubidium Vapor. Proceedings of the IEEE International Conference on Electrical Engineering and Photonics, EExPolytech 2020, pp. 248-250. DOI 10.1109/EExPolytech 50912.2020.924 3991].

**Acknowledgments:** The authors are grateful to the administration and staff of Peter the Great St. Petersburg Polytechnic University, where this work was carried out.

**Conflicts of Interest:** The authors declare no conflict of interest.

## References

1. Delva, P.; Puchades, N.; Schönemann, E.; Dilssner, F.; Courde, C.; Bertone, S.; Gonzalez, F.; Hees, A.; le Poncin-Lafitte, C.; Meynadier, F.; et al. Gravitational Redshift Test Using Eccentric Galileo Satellites. *Phys. Rev. Lett.* **2018**, *121*, 231101. [[CrossRef](#)] [[PubMed](#)]
2. Grishaev, A.A. The Doppler Second-Order Effect as a Consequence of Shift of Energy Levels of Moving Quantum Oscillators. In Proceedings of the 1998 International Symposium on Acoustoelectronics, Frequency Control and Signal Generation, Moscow/St. Petersburg, Russia, 25 April 1998; p. 33.
3. Riehle, F. *Frequency Standards: Basics and Applications*; John Wiley & Sons: Hoboken, NJ, USA, 2006.
4. Happer, W.; Mathur, B.S. Effective operator formalism in optical pumping. *Phys. Rev.* **1967**, *163*, 12–25. [[CrossRef](#)]
5. Semenov, V.V. On the contribution of the tensor component to the light shift of the frequency of radio-optical microwave resonance in rubidium vapor. *Izv. VUZov* **1999**, *2*, 86–90.
6. Baranov, A.A.; Ermak, S.V.; Sagitov, E.A.; Smolin, R.V.; Semenov, V.V. Double resonance frequency light shift compensation in optically oriented laser-pumped alkali atoms. *J. Exp. Theor. Phys.* **2015**, *121*, 393–403. [[CrossRef](#)]
7. Ermak, S.V.; Lozov, R.K.; Semenov, V.V. Orientational Light Shift Experimental Estimate of 0-0 Resonance Frequency in Rubidium Vapor. In Proceedings of the IEEE International Conference on Electrical Engineering and Photonics, EExPolytech, St. Petersburg, Russia, 15–16 October 2020; pp. 248–250.
8. Camparo, J.C.; Hagerman, J.O.; McClelland, T.A. Long-term behavior of rubidium clocks in space. In Proceedings of the European Frequency and Time Forum, Gothenburg, Sweden, 23–27 April 2012; pp. 501–508.
9. Formichella, V.; Camparo, J.; Tavella, P. Light-shift coefficient in GPS rubidium clocks: Estimation methods using lamp-light/frequency correlations. In Proceedings of the European Frequency and Time Forum (EFTF), York, UK, 4–7 April 2016; pp. 1–4.
10. Huang, M.; Stapleton, A.; Camparo, J. Lamplight Stabilization for GPS Rb Atomic Clocks via RF-Power Control. *IEEE Trans. Ultrason. Ferroelectr. Freq. Control* **2018**, *65*, 1804–1809. [[CrossRef](#)] [[PubMed](#)]
11. Donley, E.A.; Hodby, E.; Hollberg, L.; Kitching, J. Demonstration of high-performance compact magnetic shields for chip-scale atomic devices. *Rev. Sci. Instr.* **2007**, *78*, 083102. [[CrossRef](#)] [[PubMed](#)]
12. Aleksandrov, E.B.; Vershovskii, A.K. Modern radio-optical methods in quantum magnetometry. *UFN* **2009**, *179*, 605–637. [[CrossRef](#)]
13. Rachitskaya, A.P.; Tsikin, I.A. Gns integrity monitoring in case of a priori uncertainty about user's coordinates. In Proceedings of the 2018 IEEE International Conference on Electrical Engineering and Photonics EExPolytech, St. Petersburg, Russia, 22–23 October 2018; pp. 83–87.
14. Melikhova, A.P.; Tsikin, I.A. Optimum Array Processing with Unknown Attitude Parameters for GNSS Anti-Spoofing Integrity Monitoring. In Proceedings of the 41st International Conference on Telecommunications and Signal Processing, Athens, Greece, 4–6 July 2018.
15. Tsikin, I.A.; Shcherbinina, E.A. Algorithms of GNSS signal processing based on the generalized maximum likelihood criterion for attitude determination. In Proceedings of the 25th Saint Petersburg International Conference on Integrated Navigation Systems, St. Petersburg, Russia, 28–30 May 2018; pp. 1–4.
16. Melikhova, A.P.; Tsikin, I.A. Decision-making algorithms based on generalized likelihood ratio test for angle-of-arrival GNSS integrity monitoring. In Proceedings of the 25th Saint Petersburg International Conference on Integrated Navigation Systems, St. Petersburg, Russia, 28–30 May 2018; pp. 1–5.
17. Kurshin, A.V. Improving the accuracy of determining the location of GLONASS consumers by increasing the frequency of bookmarks of temporary information on satellites. *Trans. MAI Electron. J.* **2012**, *57*, 1–7.
18. Baranov, A.A.; Ermak, S.V.; Lozov, R.K.; Semenov, V.V. The Influence of the Magnetic Field Direction Variations on the Frequency Stability of a Gas Cell Atomic Clock. In Proceedings of the IEEE International Conference on Electrical Engineering and Photonics EExPolytech, St. Petersburg, Russia, 17–18 October 2019.
19. Baranov, A.A.; Ermak, S.V.; Lozov, R.K.; Semenov, V.V. Comparison of orientational error of an optically pumped quantum sensor in on-board equipment of Galileo and GPS satellite systems. *J. Phys. Conf. Series* **2019**, *1236*, 012077.
20. Baranov, A.A.; Ermak, S.V.; Lozov, R.K.; Semenov, V.V.; Ermak, O.V. The influence of the orientation frequency shift of the quantum sensor with optical pumping on the measurement of the orbit parameters of the satellites of navigation systems. *J. Radioeng.* **2018**, *12*, 5–12.